

# A Label-Free Cell Separation using Surface Acoustic Waves

Myeong Chan Jo and Rasim Guldiken, *Member, IEEE*

**Abstract**—We present two-stage microfluidic platform for a continuous label-free cell separation using surface acoustic waves. In the proposed platform, cells are first lined up at the center of the channel by using standing surface acoustic waves without introducing any external sheath flow. After focused at the center of the channel, the cells are then entered to the actual cell separation stage where the larger cell are exposed to more lateral displacement in the channel towards the pressure node due to the acoustic force differences. Consequently, different size cells are separated into multiple collection outlets. The focusing and separation of the cells can be accomplished simultaneously in the present two-stage microfluidic device. The device doesn't require the use of the sheath flow for positioning or aligning of cells. In this study, we demonstrated the separation of two different size particle streams (3 $\mu\text{m}$  and 10 $\mu\text{m}$ ) with this microfluidic platform without introducing any external sheath flow.

## I. INTRODUCTION

THE separation and sorting of cells are critical for many biological and biomedical applications including cell biology, diagnostics and therapeutics. For example, the efficient separation of human T-lymphocytes (CD4+) from whole blood is necessary for the diagnosis and treatment of HIV disease [1]. Also, the diagnostic test for malaria takes advantage of separating parasite infected red blood cells from uninfected cells [2]. Currently, there are several methods to separate cells for further analysis in clinical laboratory. One of the gold standards for conventional cell separator is flow cytometer. Most commonly used flow cytometer techniques are fluorescent activated cell sorting (FACS) and magnetic activated cell sorting (MACS). Although both FACS and MACS offer high-throughput sorting, these expensive methods are limited by the fact that the cells need to be tagged and aligned with a laser/fluorescent source for FACS and labeled with magnetic beads for MACS. However, the biochemical markers may not be available for a specific population, they may hinder differentiation, they may expand *in vitro* or *in vivo* and they introduce complexity to the system [3]. Therefore, there has been interest in label-free cell separation methods recently. The label-free techniques use the differences in an intrinsic physical property of the cells to be separated such as cell size, shape, electrical polarizability, density, electrical impedance, and hydrodynamic properties. To date various techniques for label-free separation and

sorting have been studied including deterministic lateral displacement [4, 5], sedimentation [6], optical lattice [7, 8], hydrodynamic filtration [9, 10] and dielectrophoresis [11, 12]. Recently, continuous separation of particles or cells has been performed with acoustic forces generated by ultrasonic waves. The label-free acoustic based methods are ideal cells manipulation methods for lab-on-a-chip devices because these methods offer low manufacturing cost, non-invasive operation, ability to sort a vast number of cells, and fast response [13-16]. In addition to separation by size, acoustic based methods enable separation by density, compressibility, acoustic contrast factor as well [13]. Also, it has been shown that the ultrasound does not damage cells or biological samples [17]. Recent studies demonstrated separation and manipulation of cells in microfluidic channels by using bulk acoustic wave (BAW) bonded to the substrate [18, 19, 20]. However, the generation of bulk acoustic wave requires high acoustic reflection coefficient of the microfluidic channel material. This requirement makes the bulk acoustic wave devices not applicable to many microfluidic devices made of materials with poor acoustic reflection, such as polydimethylsiloxane (PDMS) [21]. Additionally, it is difficult to integrate a bulk transducer to a microfluidic chip. Recently standing surface acoustic wave (SSAW), generated by interdigitated microelectrodes on piezoelectric substrate, has been demonstrated to manipulate E-coli and blood cells in microchannels [22]. The technique using a standing surface acoustic wave which is an acoustic wave traveling along the substrate surface works for any microchannel materials and can be easily incorporated into a multi-stage device because of its simplicity. Also, surface acoustic wave has been newly conducted to separate polystyrene microparticles [23]. Two sheath flows were used to align a particle stream and to prevent particles from trapping and aggregating along the sidewall of the channel in the device. However, introducing sheath flow to a microfluidic channel have several fundamental disadvantages such as dilution of the analyte by the sheath liquid, need for accurate flow control between the sample and sheath flow and separation efficiency strongly depending on the sheath liquid composition [24]. Most recently, cell sorting actuated by surface acoustic wave has been demonstrated [25]. However, the physical principle of the technique is based on acoustic streaming. As a result, there is a need to investigate sheathless flow methods for separating various cells in suspension by using surface acoustic waves for the development of integrated microfluidic devices. In this paper, two-stage microfluidic device for continuous cells separation using surface acoustic wave (SAW) without introducing sheath flow are presented.

Dr. Rasim Guldiken is with the Department of Mechanical Engineering, University of South Florida, Tampa, FL 33620 USA (corresponding author to provide phone: 813-974-5628; fax: 813-974-3539; e-mail: guldiken@usf.edu).

Myeong Chan Jo is with the Department of Mechanical Engineering, University of South Florida, Tampa, FL 33620 USA (e-mail: mjo@mail.usf.edu).

## II. WORKING PRINCIPLE

The force acting on the cells is as the follow [26]:

$$F_{ac} = -\left(\frac{\pi p_0^2 V_p \beta_m}{2\lambda}\right) \phi(\beta, \rho) \sin\left(\frac{4\pi x}{\lambda}\right) \quad (1)$$

where  $p_0$ ,  $\lambda$ ,  $V_p$ ,  $x$  are the acoustic pressure amplitude, wavelength, cell volume, the distance away from the pressure node respectively. Acoustic contrast factor,  $\phi$ , determines the direction of the acoustic force: if  $\phi > 0$ , cells will be attracted to the pressure node; if  $\phi < 0$ , cells will aggregate at the anti-node. Acoustic contrast factor is defined by:

$$\phi = \frac{5\rho_p - 2\rho_m}{2\rho_p + \rho_m} - \frac{\beta_p}{\beta_m} \quad (2)$$

where  $\rho_p$ ,  $\rho_m$ ,  $\beta_p$ ,  $\beta_m$  are cell density, medium density, cell compressibility and medium compressibility respectively. For example, an interesting application of acoustic separation method is the purification of blood from lipid droplets during open heart surgery. Since the lipid particles and red blood cells in blood plasma have the different sign of the acoustic contrast factor,  $\phi \approx 0.3$  and  $\phi \approx -0.3$  respectively, the acoustic force on red blood cells pushes the cells towards pressure nodes of the standing wave, whereas lipid droplets are pushed towards pressure antinodes [27]. In the present technique, there are two-stages that serve different functions within a single microfluidic channel as schematically illustrated in Figure 1. The first stage is designed to align the cells at the center of the microfluidic channel by surface acoustic waves without adding any external sheath flow. The second stage is responsible from separating the cells according to size, density, compressibility and acoustic contrast factor. The microchannel width of the first stage is designed to be half of SAW wavelength so that single pressure node coincides with the center of the channel, while the channel width of the second stage is chosen to be SAW wavelength so that the channel has two pressure nodes. For the operation of the device, two interdigitated transducer (IDT) pairs are patterned on a piezoelectric substrate and a microfluidic channel is aligned at half way between the IDT pairs. When the two IDTs are applied with a RF signal, two series of surface acoustic waves propagate in opposite directions toward the cell solution inside the microchannel. The interference of the two surface acoustic waves generates the periodic distribution of pressure nodes and anti-node on the substrate. When surface acoustic wave reach the medium, leakage waves in longitudinal mode are generated inside the medium, resulting in the pressure fluctuation. The acoustic radiation forces caused by the pressure fluctuations move the cells toward the pressure nodes or anti-nodes depending on the acoustic contrast factor. Due to the laminar flow behavior of the microfluidics flow, the cells will stay in the defined position even after the acoustic force field is removed. For size based separation, since the acoustic force is proportional to the volume of the cells, larger cells are subjected to larger acoustic force. After passing the first stage, due to this difference in magnitude of the acoustic forces acting on cells, the larger cells reaches the pressure node in less time than

does the smaller cells. As a result, the cells are repositioned with different lateral displacement along the cross-section of the channel, which is split into multiple collection outlets.

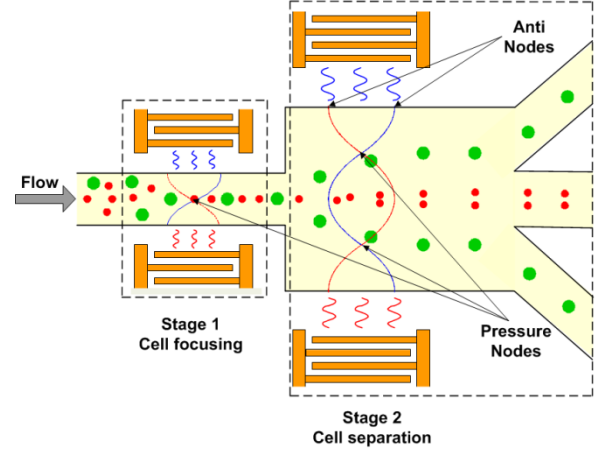


Fig. 1. Schematic diagram of the working mechanism for the two-stage cell separator using surface acoustic waves.

## III. EXPERIMENTAL SETUP

### A. Device Fabrication

The fabrication procedures for the two-stage cell separation device can be classified into three steps: the fabrication of IDTs on a piezoelectric substrate, the fabrication of a PDMS microchannel, and the bonding of the PDMS microchannel and the substrate containing IDTs. Figure 2 shows the fabrication process flow of the present cell separators. For the fabrication of IDTs on a substrate, a two-side polished Y+128° X-propagation lithium niobate (LiNbO<sub>3</sub>) wafer was used since it has a very high electromechanical coupling coefficient. The chrome layer was deposited on the lithium niobate wafer at the thickness of 1000Å using CRC sputter. The lithium niobate wafer was, then, coated with 1.6µm-thick photoresist (S1813, Shipley, Marlborough, MA), patterned with a UV light source, and developed in a photoresist developer (MF 319, Shipley, Marlborough, MA). A chrome layer was etched according to the photoresist using chrome etchant (CR-7S, Cyantek, Fremont, CA). Finally, the photoresist was removed by the PR remover. The fabricated IDTs on the lithium niobate substrate are shown in Figure 3 (a).

Next, a microchannel was fabricated with PDMS (PolyDiMethylSiloxane) micromolding technique. The mold was patterned on the silicon wafer by 100µm-thick negative photoresist (SU-8 2075, MicroChem, Newton, MA). The PDMS oligomer and crosslinking prepolymer of PDMS agent from a Sylgard™ 184 kit (Dow Corning, Midland, MI) was mixed in a weight ratio of 10:1, poured onto the SU-8 mold, and then cured at room temperature for 24hours more in order to prevent PDMS shrinking due to a heat. After PDMS replica was peeled off from the mold, the inlets and outlets were generated using the biopsy punch. The fabricated microchannel mold is shown in Figure 3 (b).

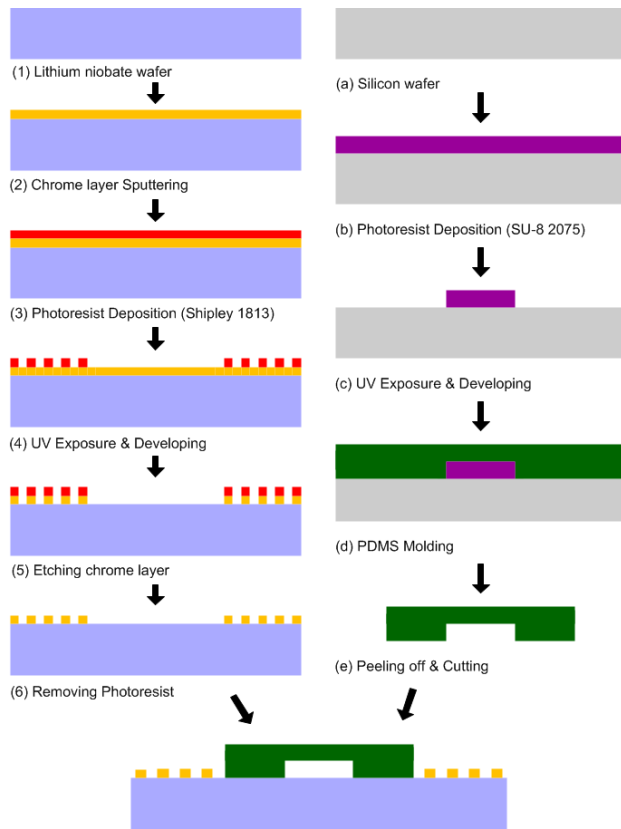


Fig. 2. Fabrication process flow of the two-stage cell separator using SAW

For the bonding a PDMS microchannel to the IDTs on a  $\text{LiNbO}_3$ , oxygen plasma was utilized to activate the both surfaces. Drops of non-swelling solvents such as ethanol were placed between activated surfaces to act as a lubricant when the alignment was accomplished manually by viewing under a microscope and to prolong the working time of oxygen plasma treatment. Alignment marks on both the microchannel and substrate is a good way to align the features accurately. To remove ethanol, the aligned device was placed in a vacuum chamber, and then PTFE tubings were connected the fabricated device to a syringe pump. Figure 4 shows the bonded two-stage microfluidic device including the PDMS microchannel and IDTs substrate.

### B. Measurement setup

In the present device, the SAW wavelength, the IDT finger pitch, and finger width are  $300\mu\text{m}$ ,  $300\mu\text{m}$ , and  $75\mu\text{m}$ , respectively. The resonance frequency of the SAW is determined by the ratio of the SAW velocity ( $V_{\text{SAW}}$ ) in the substrate and SAW wavelength ( $\lambda$ );  $f = V_{\text{SAW}}/\lambda$ . The SAW velocity is  $3970\text{m/s}$  for the chosen SAW direction on the substrate ( $\text{LiNbO}_3$ ) presented here, the resonance frequency, thus, of the SAW is  $13.2\text{MHz}$ . The microchannel width of the first stage is  $150\mu\text{m}$ , a half of SAW wavelength, to contain only one pressure node in the center of the channel. On the other hand, that of the second stage is  $300\mu\text{m}$ , the same as SAW wavelength, to hold two pressure nodes in the channel. A preliminary proof-of-concept experiment was conducted with the device on an inverted microscope (Ti-U, Nikon). A

mixture solution of polystyrene fluorescent particles (Thermo Scientific, Waltham, MA) with diameters  $3\mu\text{m}$  (red) and  $10\mu\text{m}$  diameter (green) was injected into the microchannel by a syringe pump (KDS200, KD Scientific, Holliston, MA). An AC signal was generated by a signal generator (AFG3022B, Tektronix) and then amplified by a RF power amplifier (325LA, ENI). The signal was split two ways to provide identical signals to the IDTs and generate SAWs. The power supplied to the IDTs can be adjusted such that the particles most affected by the acoustic force arrive at the center of the channel in the first stage before reaching the second stage. The process could subsequently be controlled by tuning the signal frequency, the input power, and the flow rates to achieve high separation efficiency. The net power applied to the IDTs ranged from  $250\text{mW}$  to  $1\text{W}$  and the flow rate operated was  $1\mu\text{l/min}$  to  $8\mu\text{l/min}$ . The images and a real-time video of particle focusing and separation inside the device were recorded using an inverted fluorescence microscope equipped with CCD camera.

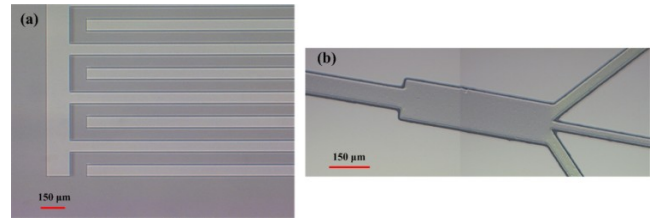


Fig. 3. (a) Fabricated IDTs patterned on lithium niobate wafer. (b) Fabricated SU-8 microchannel mold

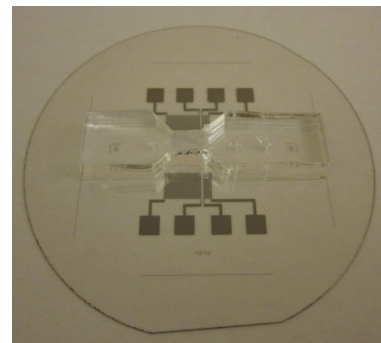


Fig. 4. The completed two-stage cell separator using surface acoustic waves.

## IV. EXPERIMENTAL RESULTS

The distribution of each particle was captured during the separation process at three different locations marked as (a), (b) and (c) in Figure 5. Location (a) was before the particles enter the first stage. One can clearly observe that both sizes particles were randomly scattered in the channel. When particles entered the first stage (location (b), the acoustic forces acting on particles aligned them at the center of the channel where pressure nodes existed. Location (c) coincided with the second stage of the device. As can be observed from Figure 5,  $10\mu\text{m}$  particles moved to the pressure nodes while  $3\mu\text{m}$  particles remained in the center of the channel because the acoustic forces exerted on the  $3\mu\text{m}$  particles were

insufficient to push them into the pressure nodes. As a result, the larger particles were separated to the side channels and the smaller particles were separated to the center channels. This significant experiment showed that the present device is capable of separating different size particles based on surface acoustic waves without introducing any external sheath flow to the microchannel.

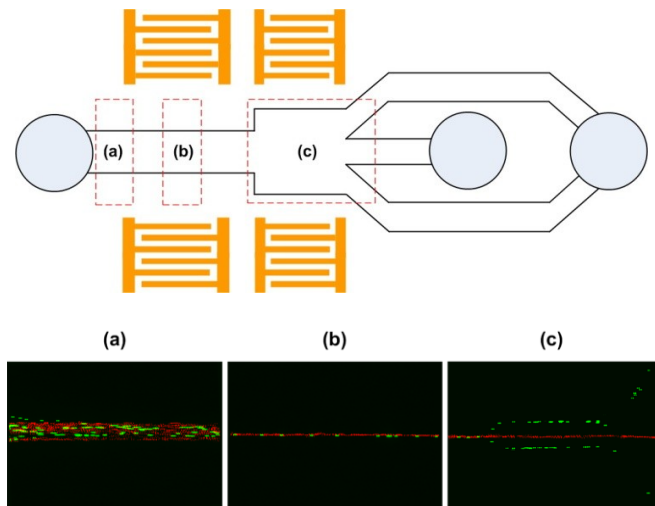


Fig. 5. Fluorescent images of the particles distribution at the chosen location (a)-(c) in the test section (green: 10µm particles, red: 3µm particles). These images were obtained with a solution containing both particle sizes, but due to the fluorescent filter requirements, the images are a composite of two images.

## V. CONCLUSION

In summary, the separation using surface acoustic wave-based two-stage microfluidic device has been demonstrated. The prominent features of the present two-stage microfluidic device are that cell focusing and separation are accomplished simultaneously and the device doesn't require the use of the sheath flow for positioning or aligning of cells. The present proof-of-concept experiments does indeed show that the proposed concept works as hypothesized with the non-optimized preliminary device. We will conduct the design optimization studies with the advanced simulation and theoretical analysis as well as similar characterization experiments to obtain separation efficiency among other significant parameters. We expect that two-stage cell separator using surface acoustic waves can be used in a wide variety of biological and biomedical applications.

## REFERENCES

- [1] X. Cheng, D. Irimia, M. Dixon, K. Sekine, U. Demirci, L. Zamir, R. G. Tompkins, W. Rodriguez, and M. Toner, "A microfluidic device for practical label-free CD4 + T cell counting of HIV-infected subjects," *Lab Chip*, vol. 7, pp. 170–178, 2007.
- [2] P. Gascoyne, J. Satayavivad, and M. Ruchirawat, "Microfluidic approaches to malaria detection," *Acta Tropica*, vol. 89, pp. 357–369, 2004.
- [3] B. Roda, P. Reschiglian, A. Zattoni, F. Alviano, G. Lanzoni, R. Costa, A. Di Carlo, C. Marchionni, M. Franchina, L. Bonsi, and G. P. Bagnara, "A tag-less method of sorting stem cells from clinical specimens and separating mesenchymal from epithelial progenitor cells," *Cytometry B Clin Cytom*, vol. 76B, pp. 285–290, 2009.
- [4] L. Huang, E. Cox, R. Austin, and J. Sturm, "Continuous particle separation through deterministic lateral displacement," *Science*, vol. 304, pp. 987–990, 2004.
- [5] B. R. Long, M. Heller, J. P. Beech, H. Linke, H. Bruus, and J. O. Tegenfeldt, "Multidirectional sorting modes in deterministic lateral displacement devices," *Phys Rev E*, vol. 78, pp. 046304–046309, 2008.
- [6] D. Huh, J. H. Bahng, Y. Ling, H. H. Wei, O. D. Kripfgans, J. B. Fowlkes, J. B. Grotberg, and S. Takayama, "Gravity-driven microfluidic particle sorting device with hydrodynamic separation amplification," *Anal Chem*, vol. 79, pp. 1369–1376, 2007.
- [7] M. MacDonald, G. Spalding, and K. Dholakia, "Microfluidic sorting in an optical lattice," *Nature*, vol. 426, pp. 421–424, 2003.
- [8] A. T. Ohta, P. Chiou, H. L. Phan, S. W. Sherwood, J. M. Yang, A. N. K. Lau, H. Y. Hsu, A. Jamshidi, and M. C. Wu, "Optically controlled cell discrimination and trapping using optoelectronic tweezers," *IEEE J Sel Top Quantum Electron*, vol. 13, pp. 235–243, 2007.
- [9] M. Yamada and M. Seki, "Hydrodynamic filtration for on-chip particle concentration and classification utilizing microfluidics," *Lab Chip*, vol. 5, pp. 1233–1239, 2005.
- [10] M. Yamada, K. Kano, Y. Tsuda, J. Kobayashi, M. Yamato, M. Seki, and T. Okano, "Microfluidic devices for size-dependent separation of liver cells," *Biomed Microdevices*, vol. 9, pp. 637–645, 2007.
- [11] P. R. C. Gascoyne and J. Vykoukal, "Particle separation by dielectrophoresis," *Electrophoresis*, vol. 23, pp. 1973–1983, 2002.
- [12] I. Cheng, V. E. Froude, Y. Zhu, and H. Chang, "A continuous high-throughput bioparticle sorter based on 3D traveling-wave dielectrophoresis," *Lab Chip*, vol. 9, pp. 3193–3201, 2009.
- [13] S. Kapishnikov, V. Kantsler, and V. Steinberg, "Continuous particle size separation and size sorting using ultrasound in a microchannel," *J. Stat. Mech.*, P01012, 2006.
- [14] A. Nilsson, F. Petersson, H. Jönsson, and T. Laurell, "Acoustic control of suspended particles in micro fluidic chips," *Lab Chip*, vol. 4, pp. 131–135, 2004.
- [15] J. Shi, X. Mao, D. Ahmed, A. Colletti, T. J. Huang, "Focusing microparticles in a microfluidic channel with standing surface acoustic waves (SSAW)," *Lab Chip*, vol. 8, pp. 221–223, 2008.
- [16] M. Wiklund, C. Günther, R. Lemor, M. Jäger, G. Fuhr, and H. M. Hertz, "Ultrasonic standing wave manipulation technology integrated into a dielectrophoretic chip," *Lab Chip*, vol. 6, pp. 1537–1544, 2006.
- [17] F. S. Foster, C. J. Pavlin, K. A. Harasiewicz, D. A. Christopher, and D. H. Turnbull, "Advances in ultrasound biomicroscopy," *Ultrasound Med. Biol.*, vol. 26, pp. 1–27, 2000.
- [18] F. Petersson, A. Lena, A. Sward-Nilsson, and T. Laurell, "Free flow acoustophoresis: Microfluidic-based mode of particle and cell separation," *Anal Chem*, vol. 79, pp. 5117–5123, 2007.
- [19] H. Jonsson, C. Holm, A. Nilsson, F. Petersson, P. Johnson, and T. Laurell, "Particle separation using ultrasound can radically reduce embolic load to brain after cardiac surgery," *Ann Thorac Surg*, vol. 78, pp. 1572–1578, 2004.
- [20] T. Laurell, F. Petersson, and A. Nilsson, "Chip integrated strategies for acoustic separation and manipulation of cells and particles," *Chem. Soc. Rev.*, vol. 36, pp. 492–506, 2007.
- [21] J. Shi, X. Mao, D. Ahmed, A. Colletti, and T. J. Huang, "Focusing microparticles in a microfluidic channel with standing surface acoustic waves (SSAW)," *Lab Chip*, vol. 8, pp. 221–223, 2008.
- [22] J. Shi, D. Ahmed, X. Mao, S. S. Lin, A. Lawit, and T. J. Huang, "Acoustic tweezers: patterning cells and microparticles using standing surface acoustic waves (SSAW)," *Lab Chip*, vol. 9, pp. 2890–2895, 2009.
- [23] J. Shi, H. Huang, Z. Stratton, Y. Huang, and T. J. Huang, "Continuous particle separation in a microfluidic channel via standing surface acoustic waves (SSAW)," *Lab Chip*, vol. 9, pp. 3354–3359, 2009.
- [24] M. A. Strega and A. Lagu, *Capillary Electrophoresis of Proteins and Peptides*, New Jersey: Humana Press, 2004.
- [25] T. Franke, S. Braunmüller, L. Schmid, A. Wixforth, and D. A. Weitz, "Surface acoustic wave actuated cell sorting (SAWACS)," *Lab Chip*, vol. 10, pp. 789–794, 2010.
- [26] K. Yosioka and Y. Kawasima, "Acoustic radiation pressure on a compressible sphere," *Acustica*, vol. 5, pp. 167–173, 1955.
- [27] F. Petersson, A. Nilsson, C. Holm, H. Jonsson, and T. Laurell, "Separation of lipids from blood utilizing ultrasonic standing waves in microfluidic channels," *Analyst*, vol. 129, pp. 938–943, 2004.